Observed Behaviours in Simulated Close-range Pedestrian Dynamics

Omar Hesham, Princy, Walter Aburime, Ziyad Rabeh, Shashi Bhushan and Gabriel Wainer

Carleton University
Department of Systems and Computer Engineering
{omarhesham, princyprincy, walteraburime, ziyadrabeh, shashibhushan}@cmail.carleton.ca,
gwainer@sce.carleton.ca

ABSTRACT

Crowd simulation can be a useful tool for predicting, analyzing, and planning mass-gathering events. The analysis of simulated crowds aims to extract observations to assess occupant interactions and potential crowd flow issues. This paper presents a continuous-space definition of Centroidal Particle Dynamics (CPD) crowd models, then proceeds to present behaviours observed in the simulated crowds. These include organized micro-grouping (flocking), uncooperative behaviors like passage blocking and collisions due to distracted pedestrians. It also briefly explores how spatial design choices could positively impact pedestrian flow. The observations might be of interest to designers of urban and architectural spaces who are looking to improve pedestrian or occupant experience, particularly in high-density crowd scenarios. The presented CPD method is additionally implemented to run on mobile (Android) devices, allowing on-the-field crowd simulation for event planning.

Author Keywords

Occupant simulation; crowd analysis; emergent behaviour; interactive frame-rate; agent-based pedestrian dynamics.

ACM Classification Keywords

I.6.5 [SIMULATION AND MODELING]: Model Development; I.3.7 [COMPUTER GRAPHICS]: Animation.

1   INTRODUCTION

We simulate close-range crowd behaviour using a personal space preserving method, known as the Centroidal Particle Dynamics (CPD) method [1]. As a variant of the social forces model [2], the CPD method models close-range interactions of pedestrians by explicitly asking them to maintain and regain their personal space in their vicinity. In high-density crowd scenarios, the concept of personal space preservation seems to produce believable results. This intangible concept of "personal space" has biological origins, namely the Amygdala, the fear center of the brain [3]. That is to say that the preservation of personal space (~0.8m-1m) is a fear response. Particularly, it's a mechanism for subconsciously affording us a buffer of time to react to negative outcomes, especially near strangers. The specific distance varies across cultures and social settings, but the biological origin explains the near universal range of (~0.8-1m).

2   CROWD INTERACTION MODEL

An overview of the CPD method is shown in Figure 1. We start by using the entity (pedestrian) positions to construct a Personal Space Map (PSM). This map is a global operation that explicitly maps out the current personal space (PS) of each entity in the scene. Each pedestrian can then examine the local area in their immediate surrounding (~0.8m-1m) to calculate how much of their personal space was violated and the appropriate response. This is done by computing the new geometric center (or centroid) of the currently available personal space. A vector pointing the pedestrian to this new centroid is called the Centroidal Force. In essence, this force, if followed, will allow the pedestrian to regain the most amount of personal space.

Once the local (centroidal) force is computed, it is integrated with other relevant forces to the pedestrian (e.g. global path, friction, maintaining proximity to nearby family members). Such forces can be given weights, which can be treated as the parameters of the overall pedestrian simulation. As we will see throughout the experiments in Sections 3-5, modifying these parameters will result in different emergent behaviours. Lastly, the acceleration a_t experienced by the pedestrian (due to the net force) at time t is finally integrated using a time solver. We opt for a Verlet (Symplectic) solver as a happy medium between an explicit solver's computational speed, and an implicit solver's energy conservation. The integration of pedestrian position p over timestep δt is given by:

$$p_{t+\delta t} = 2p_t - p_{t-\delta t} + \delta t^2 a_t$$
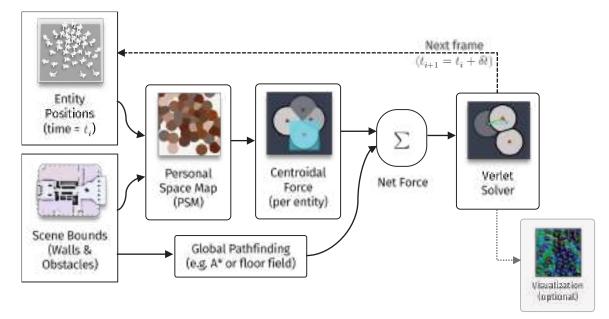
Figure 1. Overview of pedestrian update cycle per time frame (δt).

Symplectic solvers are popular in video games and in real-time physics engines. We point the interested reader to [4] and [5] for more on this optimization topic.

2.1 PSM Construction

The PSM is defined as a tessellation or partitioning of a 2D plane G (i.e. the ground) on which scene obstacles exist (walls, gates, barriers, parked vehicles, etc.) and pedestrians traverse. After the PSM construction is done, every point g in plane G, will belong to one and only one entity (e.g. pedestrian_13, obstacle, or unoccupied space). Let T denote the many-to-one mapping that tessellates plane G.

To start, all points $g \in G$ are considered *unoccupied* (or numerically 0) to represent all the empty space available for any pedestrian to traverse:

$$T(g) = 0, \quad \text{for all } g \in G.$$

CPD pedestrians will be accounted for by performing a constrained Voronoi tessellation with pedestrian positions as the Voronoi sites, and the personal space (PS) radius as the constraint. Let's assume that each pedestrian is assigned a unique identifier from 1 to n. If we denote $d(a,b)$ as the Euclidean distance between any two points a and b on plane G, then the tessellation now becomes:

$$T(g) = \begin{cases} i, & (d(g,p_i) < r_i) \ \wedge \ (d(g,p_i) < d(g,p_j)) \ \forall \ i \neq j \\ 0, & \text{otherwise} \end{cases},$$

where $i, j \in \{1, \ldots, n\}$; p_i is the position of pedestrian i, and r_i is the radius of pedestrian i's personal space (PS).

Finally, scene obstacles can be explicitly defined by the modeler, for example set $B \subset G$ which denotes areas that the

pedestrian needs to avoid. Additionally, scene geometry can be projected onto G as if viewed orthogonally from the top. Most scene geometry is already in 2D form (e.g. architectural floor plans), but any 3D geometry (e.g. columns or vehicles) would need to be explicitly projected onto the PSM for ground-level collision avoidance. To project 3D meshes onto G, the following transform can be applied per vertex:

$$Proj_G(v) = v - (\vec{n}_G \cdot v) \times \ v$$

Where $\vec{n}_G$ is the plane's unit normal vector, and $v = (v_x, v_y, v_z)$ is a vertex position that has a height v_y between 0m (ground) and 3m (reasonable max human height), and does not explicitly belong to a ceiling element. Then, for every point $g \in G$ that falls within the polygons formed by $Proj_G(v)$, we set $g \in B$. Hence, the set B contains all the boundary points in space G that were defined explicitly by the modeler along with all the 3d scene obstacle projections. When tessellating G, we -currently- don't explicitly differentiate between different obstacles, and hence assign them the same value *obstacle* (or numerically -1):

$$T(g) = \begin{cases} i, & (d(g,p_i) < r_i) \ \wedge \ (d(g,p_i) < d(g,p_j)) \ \wedge \ g \notin B \\ -1, & \text{for all } g \in B \\ 0, & \text{otherwise} \end{cases},$$

The entire PSM tessellation process is memoryless and gets reconstructed every time step in the same fashion. In doing so, the PSM can account for dynamic obstacles in the scene, such as revolving doors.

The projection step allows us to accommodate basic inclines, but more work needs to be done to extend the PSM to allow for uneven terrain, stairs, and multi-story evacuation.

2.2 Global Pathfinding

In addition to the local avoidance maneuvers that pedestrians perform to maintain their personal space, they typically also have a global target location that they're trying to get to.

Classic path-finding methods can be deployed here to find the optimal path the pedestrian needs to travel to reach its target. If the scene obstacles are defined over a graph, then a method like A* path finding [6] would work well in our real-time environment, as it efficiently computes such global paths per entity and can be updated every reasonable interval (say 5 seconds) throughout the simulation. But for large scale simulations involving thousands of pedestrians with relatively few possible global targets within the scene (e.g. only dozens of shops within an event, as shown in Figure 2), a single global floor map per target is more computationally efficient. The map is essentially a 2D gradient field that points an entity to the direction it needs to follow to reach the global target. See [7], [8] for example implementations of this floor field.

2.3 Net Force

Regardless of the method used, the global path force vector is part of the net force calculation experienced by each pedestrian (Figure 1). The net force calculation will be:

$$nf_i = \alpha\ cf_i + \beta\ gf(p_i) + \gamma\ uf_i,$$

where $gf(p_i)$ is the global path vector given pedestrian i's current position in the scene; and α, β, and γ are scalar weights to parametrize the overall behaviour of the entity. For instance, an aggressive pedestrian might have low α and high β values, hence emphasizing their own global path with little regard for local PS violations (indicated by the centroidal force cf_i). The force uf_i is the entity's resistance to non-optimal pathing, as presented in [9]. These parameters allow the pedestrian's behaviour to be tuned and calibrated according to input data (e.g. cultural variances). At this current stage, we empirically arrived at a default set of parameter values: $\alpha = 0.9$; $\beta = 0.25$; and $\gamma = 0.1$.

Figure 2. Crowded event with dense, predominantly bidirectional, pedestrian traffic (Oktoberfest, Munich. Intrepix/shutterstock.com)

3 OBSERVED BEHAVIOURS IN SIMULATED CROWDS

We're primarily concerned with simulating densely crowded scenarios where crowd planning/management is important. These can range from socially festive events such as sports and concerts, to politically-oriented and religious events. If crowd density is not properly managed, these otherwise peaceful gatherings could result in unintended crowd crushes or stampedes with tragic results [10]. Our hope is to "make contributions to the growing body of literature regarding crowd dynamics", one of the central recommendations in [10] to support safer mass gatherings. The method and tools presented here could further facilitate the inclusion of architecture and urban design(ers) as solution vectors for this critical issue rather than leaning heavily on law enforcement and on-site crowd control measures. A "prevention (through good design) is better than cure" kind of approach.

Section 3 will attempt to provide preliminary validation for the presented CPD method through cursory comparison against real-data. Later sections will extrapolate this knowledge to derive results and insights from a few purely simulated scenarios.

3.1 Bidirectional Flow

When explicit lanes and barriers are not specified, a bidirectional stream of pedestrians sharing the same space will eventually form lanes on their own. These organically-emergent lanes reduce friction between the opposing streams. Figure 3 shows a video footage capture from a bidirectional experiment [11], and alongside it is the CPD simulation. The red-coded people are headed west, while the black-coded ones are headed east. Similarly, the red-coded simulated pedestrians are headed west, while the blue-coded ones are headed east. The simulation displays similar density changes across simulation time (low to high to low again). Of note is the "fan-out" effect seen towards the end of the stream, where entities finally have the space to regain their personal space, and immediately spread out. This effect is also seen in the simulation (bottom right corner in Figure 3).
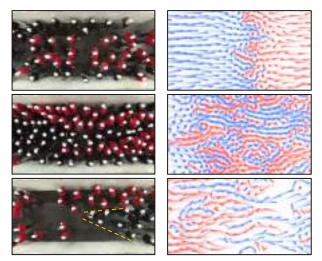

Figure 3. Our simulated crowd (right) compared to a real bidirectional scenario. Time progresses from top to bottom.
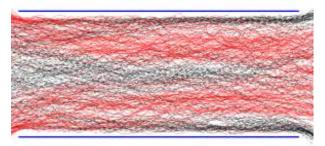
Figure 4. Trace of all pedestrian trajectories from the real bidirectional footage in Figure 3.

Figure 4, obtained from [12], is a trace of the trajectory of bidirectional flow of the reference footage shown in Figure 3. The emergent lane formation is clearly apparent from this trace. The corridor in the footage was 3.6m wide. Larger-sized experiments are difficult to construct and coordinate (e.g. this narrow corridor experiment required over 300 volunteers). So, one can imagine that data capture of a bigger bidirectional flow scenario (like in Figure 2) under controlled lab conditions would be difficult.

Simulation can become a useful tool here. We extrapolated the CPD bidirectional scenario by simulating a much wider 20m virtual corridor. The trace shown in Figure 5 illustrates how the model was able to maintain lane formation patterns, comparable to the pattern observed in reality (Figure 4), thus facilitating the study (and crowd planning) for larger events such as the busy bidirectional street shown in Figure 2.
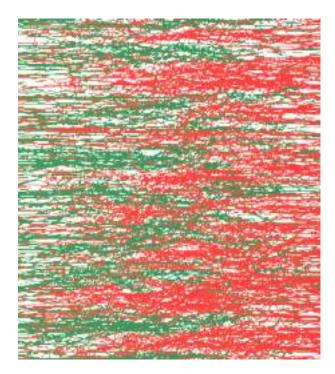

Figure 5. Trace of the emergent lane formation by virtual pedestrians simulated in a wide corridor.

4 UNCOOPERATIVE BEHAVIOUR

The ideal pedestrian would pay attention all the time to their surroundings. By pre-emptively and carefully retaining their personal space, they should be able to avoid most collisions and disruptions to their intended motion. We see such efficiencies in busy crossings, such as Shibuya, Japan, where hundreds of pedestrians with competing trajectories are able to cross smoothly.

However, we also simulated a few behaviours that would be deemed uncooperative to the collective pedestrian motion, effectively disrupting it. Again, there is a lack of controlled experiments that capture motion data from such scenarios, so we rely on the strength of CPD illustrated so far.

4.1 Passage Blocking

Unlike clearly visible and static obstacles in the scene (e.g. wall, vegetation, park benches, etc.), static subgroups in the crowd can be more difficult detect in a dense scenario until very close to that group. Figure 6 shows a bidirectional scenario in a 3.5m hallway. We assign a few pedestrians to stand still, effectively blocking passage. As expected the time it takes the other pedestrians to cross is increased. When a much wider 40m corridor was simulated, as shown in Figure 7 (think a busy path on a campus, or access to cafeteria area), an interesting observation arose. As expected, the are surrounding the uncooperative bunch (bright green) experienced congestion. However, later in the simulation, we observed multiple pockets of congestion forming away from the initial bundle. These secondary masses of congestion result from the diverted traffic concentrating on the new limited space. The insight here is that even if the width of passage is much wider than the uncooperating group, a high pedestrian flow rate will cause pockets of congestion to inevitably form across the width of the corridor.
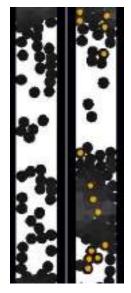

Figure 6. In narrow hallways, a few pedestrians standing still (e.g. chatting, etc.) could cause significant congestion. Left: entities standing still (yellow); Right: same simulation time instance with no entities blocking the hallway.
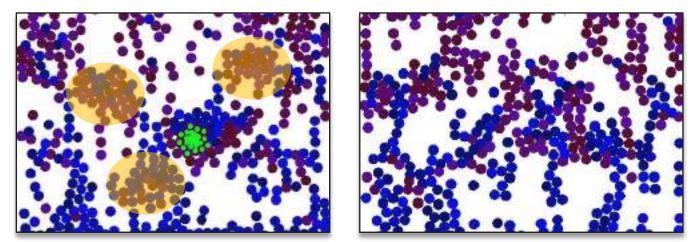
168

Figure 7. A north-south bound (red-blue) bidirectional flow. Left: entities disrupting the flow by standing still (shown in green) lead to pockets of congestion across the entire corridor within a few of minutes. Right: an unimpeded corridor captured at the same simulation time as the left scenario; here, lane formation across the full width (~40m) resulted in a more spread-out distribution of density, while having already let more people pass through at that point in simulation time.

4.2 Distracted Pedestrians

Distracted pedestrians can cause injury to themselves and others. Large events, as depicted in Figure 2, are tricky to navigate as it is and the possibility for slight collision (shoulder rubbing) is not hard to imagine. So, we wanted to simulate how distracted pedestrians might make navigating such events even harder. The most common cause or manifestation of this distracted behaviour is pedestrians texting/browsing on their phone. Our models were setup for distracted pedestrians as follows:

- Distraction period: 5 seconds every 15 seconds (~third of their time distracted on their phone).

- Speed slows down to 40% [13]; and the PS weight map is culled to match the reduced visibility ahead of the distracted entity, as shown in Figure 8.

Figure 9 illustrates the scene setup while Figure 10 charts a sample of collision counts recorded. In the absence of any distracted pedestrians, only a handful of instances of high collision likelihood have been observed. The count increases exponentially as the ratio of distracted entities increases within the dense crowd. These collisions count were also
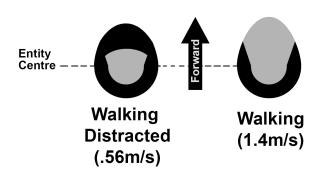

Figure 9. An example of 30% distracted pedestrians in north-south bidirectional flow. Red indicates detected instance of high likelihood of collision. Orange indicates all distracted pedestrians.

inversely proportional to corridor width; not due to increased bidirectional flow density, but rather due to the lack of additional space for undistracted pedestrians to perform their avoidance maneuvers. Collisions counts were much less pronounced in unidirectional flow, where the biggest effect was instead the slowdown of surrounding entity motion. This can be explained by the fact that relative velocities between the entities are on-average less than the relative velocities in bidirectional flow, which gives fully-aware entities a larger amount of time to react and manoeuvre around the distracted crowd when needed.

Figure 8. The personal space (PS) weight map for a pedestrian distracted on their phone (left) is culled from the front due to lack of visibility, in contrast to a normally walking CPD kernel from [9].
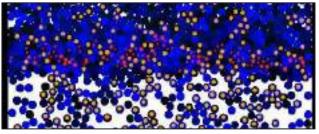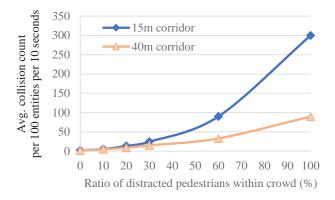

Figure 10. Collision counts recorded from scenario in Figure 9.

5 ORGANIZED GROUPING

Up to this point, we've assumed that entities are entirely individualistic with little to no relation between them; and we saw how phenomenon like lane formation which appear to be organized are in fact just emergent global behaviours due to each entity pursuing entirely individualistic pedestrian dynamics. In this section, we examine scenarios that involve intentional organization. For example, pedestrians travelling in groups (e.g. tourists in a tour group, or a family staying close together at a crowded festival). In those cases, the entities require additional social forces to be accounted for when computing each entity's net force. But we note that personal space (centroidal) forces don't change just because people have organized into groups; every entity still wants to maintain a reasonable personal space within its surrounding.

The difficulty in pursuing such experiments is the lack of real data on micro-grouping configurations, especially from controlled experiments, to help us calibrate and further validate the simulated results. Such large-scale crowd data capture projects are in demand.

5.1 Disruptive Flocking
In this scenario, a crowd of 990 entities is in bidirectional flow through a 40m corridor. Ten special entities are then grouped by implementing Boids flocking rules [14] of separation, cohesion, and alignment. These forces are fed to the special entities' net force calculation (from Figure 1).

The special group underwent two simulation tasks:

   a) Starting from the sideline, the group is asked to move *across* the bidirectional stream to reach the opposite end together. (as shown in Figure 11).

   b) Starting from the north, the group is asked to move *along* the bidirectional stream to reach the south.

The average time it took the group to complete task a) is 83.75 seconds. Task b) took 68 seconds. This confirms the intuitive notion that going across the established flow of a dense crowd will be slower, as the group has to either wait for openings to cross or force their way to disrupt the bidirectional flow. While opposing flow enjoyed lane formation as an emergent optimization strategy, micro-groups flocking across the corridor did not display any particular flow-optimizing behaviour, further explaining the delay in performing task (a).

The disparity between tasks (a) and (b) did not noticeably change for larger micro-groups of more than ten individuals, however, as the groups got smaller, nearing individualistic behaviour, the disparity between the two tasks was significantly reduced, and almost imperceptible in groups of two. The immediately observable explanation is that smaller groups can seize on smaller "openings" available to cross amidst the dense crowd. Additionally, task (b) is limited by the emergent bidirectional flow rate, which at high enough densities effectively equalizes movement speed for large portions of the crowd. In other words, even through task (b)
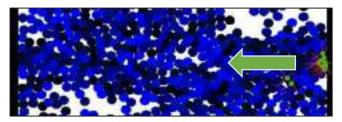

Figure 11. The ten grouped entities (green-coded) are explicitly grouped to stay together using the Boids flocking rules as they traverse across the scene (task (a)). The rest of the crowd is in north-south bidirectional motion.

seems easier, overtaking people ahead of you in a very dense crowd is quite difficult; hence the reduction in disparity between tasks (a) and (b).

5.2 Competitive Pathing
In this section, we demonstrate an experiment that illustrates the potential for architectural/urban design to address dense-crowd issues.

The scenario is an artificial setup, where entities are initially arranged equally around a ring. Each entity's target is to arrive at the opposite side of the ring. There are no other global paths and no organized grouping. This artificial setup is designed to test an algorithm's ability to handle the least optimal configuration: all pedestrians are headed into each other, and all are competing for the center of the ring to reach the other side in the shortest path possible. Such scenarios are not too far off from reality. Indeed, major crossing such as Shibuya Crossing in Japan can display such a massively competitive pedestrian scenario.

Figure 12 shows the results of the crowd motion at various time instances. Recall that the default parameter values were: $\alpha = 0.9$; $\beta = 0.25$; and $\gamma = 0.1$. We created 3 variations of the crowd, as shown in Figure 12:

  a) High aggression: $\alpha = 0.7$; $\beta = 0.3$; $\gamma = 0.4$. Here, the entities display higher-than-default drive towards the final destination (β) and lesser regard for the personal space violations (α). Additionally, the entities are highly resistant (γ) to paths that deviate from the optimal route (i.e. straight through the center of the ring). Hence, we see heavy congestion and a pattern where the red entities pierce through the blue entities to get to the other side. All entities share the same parameters; the colors only there to help visualize the overall effect.

   • Avg. density experienced by all entities: 0.3 ped/ft^2
   • Peak density: $0.8 \text{ pedestrians/ft}^2$

  b) Low aggression: $\alpha = 0.8$; $\beta = 0.2$; $\gamma = 0.1$. Here, the entities display higher regard for personal space violations than the aggressive entities in (a). They're also more receptive to deviating from the optimal path.

   • Avg. density experienced by all entities: 0.3 ped/ft^2
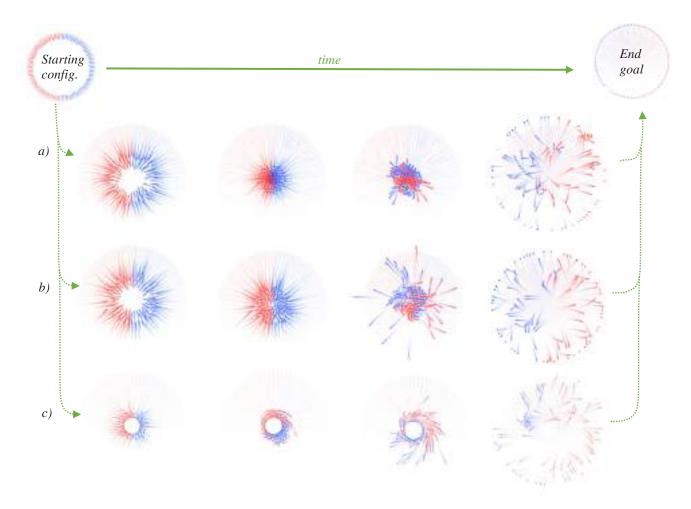   • Peak density: $0.7 \text{ pedestrians/ft}^2$

Figure 12. Concentric crowd motion under different parameter values: a) aggressive crowd; b) low aggression crowd; and c) round architectural artifact at the center of the ring with a low aggression crowd.

c) A round obstacle is inserted at the center of the ring, with the entities maintaining their low aggression parameters.

- Avg. density experienced by all entities: $0.3 \ \mathrm{ped/ft^2}$
- Peak density: $0.5 \ \mathrm{pedestrians/ft^2}$

As if guided by this new obstacle, a cyclone pattern quickly forms and facilitates the crowd's motion. It might be counter-intuitive to think that an obstacle would ease traffic, but this is an example where architectural design can experiment with ways to help guide flow without explicitly designating single-way lanes. This scenario could easily be a high-traffic zone in a busy mall, and the obstacle could be a seating area. One can imagine that this experiment could be automated through an optimization or artificial neural network (ANN) algorithm to find the optimal obstacle shape(s) for each setting.

We're additionally exploring the ability to run the simulation on mobile platforms. The idea is to empower contingency and event planners with simulation on-the-field. The CPD algorithm has been ported to run on Android (Java +

OpenGL). Figure 13 shows a demo app running CPD crowds on a Nexus 6P.

Videos of all experiments presented in this paper are made available at: http://cell-devs.sce.carleton.ca/publications/

6 CONCLUSION

Crowd simulation can be a powerful tool when planning for large-scale gatherings (e.g. concerts, sports events) and when
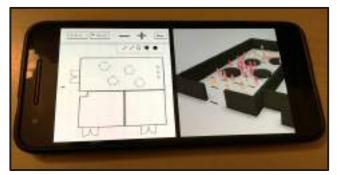

Figure 13. Demo of CPD running on Android; providing on-site scenario testing for event planners. It uses low-poly 3D character sprites, color-coded to indicate pedestrian density.

designing highly-trafficked pathways (e.g. in public transit stations). This paper presented details of the Centroidal Particle Dynamics (CPD) method in continuous form, and discussed behaviours observed in simulated crowds.

We saw how periodically distracted pedestrians (e.g. on their phone) cause a non-linear increase in the frequency of accidental collision among dense crowds in bidirectional flow corridors. These experiments might be further extended to study specific pedestrian crosswalks, where cell-phone distractions increase the risk of severe injury with vehicles nearby. Indeed, there is an ongoing debate in several cities across Canada to consider banning the use of cell phones while crossing the street. Data-driven experiments on virtual crowds could contribute to such a discussion.

Experiments on passage blocking by individuals in bidirectional flow have demonstrated how congestion can propagate across the width of a corridor, as the crowd slowly reacts to the reduced space available to self-organize into bidirectional lanes. This is an interesting phenomenon that warrants further detailed studies into the relationship between corridor width and congestion potential due to uncooperative individuals. The takeaway here is that increasing the width alone might not be a sufficient solution to reduce congestion propagation issues. Perhaps future experiments with more nuanced spatial design strategies could point to better solutions for congestion dissipation.

Further validation efforts are warranted, especially when discussing the use of simulation for safety and contingency planning. As demonstrated in this paper, CPD is quite capable of reproducing the subtle details of emergent phenomenon in dense crowd scenarios (e.g. "fanning out" in Figure 3), and extrapolating pedestrian motion data collected from lab experiments to simulate much wider areas with higher crowd counts. However, there is still room for more rigorous validation against statistical crowd motion data. We've highlighted how controlled lab experiments are rare for larger crowd counts (thousands of entities and more), and how footage analysis is often reduced to macroscopic or aggregated statistical measures. So, we look forward to improvements in computer vision techniques that can trace the microscopic motion paths for individuals in a dense crowd, or at least capture detailed statistical measures related to their microscopic behaviour.

In the end, virtual crowds are only a tool. Simulation is meant to complement, not replace, existing wisdom, experience, field studies, and analytical computations. This additional tool facilitates design iteration and visualization; and might help highlight previously unforeseen problem areas that warrant further investigation, if necessary.

ACKNOWLEDGMENTS

REFERENCES

[1] O. Hesham and G. Wainer, "Centroidal Particles for Interactive Crowd Simulation," *Proceedings of the Summer Computer Simulation Conference*. Society for Computer Simulation International, p. 7:1-7:8, 2016.

[2] D. Helbing, I. Farkas, and T. Vicsek, "Simulating dynamical features of escape panic," *Nature*, vol. 407, no. 6803, pp. 487–490, May 2000.

[3] D. P. Kennedy, J. Gläscher, J. M. Tyszka, and R. Adolphs, "Personal Space Regulation by the Human Amygdala," *Nat. Neurosci.*, vol. 12, no. 10, pp. 1226–1227, 2010.

[4] G. Van Den Bergen and D. Gregorius, *Game Physics Pearls*. 2010.

[5] K. Erleben, *Physics-based animation*. 2005.

[6] W. Zeng and R. L. Church, "Finding shortest paths on real road networks: the case for A*" *Int. J. Geogr. Inf. Sci.*, vol. 23, no. 4, pp. 531–543, Apr. 2009.

[7] A. Treuille, S. Cooper, and Z. Popović, "Continuum Crowds," *ACM Trans. Graph.*, vol. 25, no. 3, pp. 1160–1168, 2006.

[8] S. Bandini, M. Mondini, and G. Vizzari, "Modelling negative interactions among pedestrians in high density situations," *Transp. Res. Part C Emerg. Technol.*, vol. 40, pp. 251–270, 2014.

[9] O. Hesham and G. Wainer, "Context-sensitive Personal Space for Dense Crowd Simulation," in *Proceedings of the Symposium for Architecture and Urban Design*, 2017, pp. 173–180.

[10] S. A. Turris, A. Lund, and R. R. Bowles, "An analysis of mass casualty incidents in the setting of mass gatherings and special events," *Disaster Med. Public Health Prep.*, vol. 8, no. 2, pp. 143–149, 2014.

[11] J. Zhang, W. Klingsch, A. Schadschneider, and A. Seyfried, "Ordering in bidirectional pedestrian flows and its influence on the fundamental diagram," *J. Stat. Mech.*, vol. 2012, no. 2, p. P02002, 2012.

[12] J. Zhang and A. Seyfried, "Empirical Characteristics of Different Types of Pedestrian Streams," *Procedia Eng.*, vol. 62, pp. 655–662, 2013.

[13] L. L. Thompson, F. P. Rivara, R. C. Ayyagari, and B. E. Ebel, "Impact of social and technological distraction on pedestrian crossing behaviour: An observational study," *Inj. Prev.*, vol. 19, no. 4, pp. 232–237, 2013.

[14] C. W. Reynolds, "Steering behaviors for autonomous characters," *Game Developers Conference*, vol. 1999. pp. 763–782, 1999.